arXiv:2311.18597v1 [math.DS] 30 Nov 2023

Internal noise interference in anticipation of tipping points of generic multi-dimensional dynamical systems

Andreas Morr*[†] [‡], Niklas Boers[†] [‡] [§], and Peter Ashwin[§]

Abstract. A deterministic complex system that slowly passes through a generic fold-type (saddle-node) bifurcation can be reduced to one-dimensional dynamics close to the bifurcation because of the centre manifold theorem. It is often tacitly assumed that the same is true in the presence of stochasticity or noise so that, for example, critical slowing down (CSD) indicators can be applied as if the system were one-dimensional. In this work, we show that this may not be the case; specifically, we demonstrate that noise in other dimensions may interfere with indicators of CSD, also referred to as early warning signals (EWS). We point out a generic mechanism by which both variance and AC(1), as well as other EWS, can fail to signal an approaching bifurcation. This can in principle occur whenever one noise source drives multiple components of the system simultaneously. Even under the favourable assumptions of uncoupled deterministic dynamics and stationary noise, observables of the system can then exhibit false negative or false positive CSD indications. We isolate this phenomenon in an example that represents a generic two-dimensional fold-type bifurcation setting.

Key words. Abrupt transitions, Critical Slowing Down, Early Warning Signals, Multi-dimensional systems

MSC codes. 37G10, 37H05, 37H20

1. Introduction.

Many physical systems exhibit abrupt transitions or are suspected to harbour the potential for them [22, 1, 16, 28, 5, 23]. There has been an increased interest in the analysis and detection of bifurcation-induced transitions [6, 4, 8, 9, 26, 12]. Such events occur if the system's current equilibrium state vanishes in response to an external change to the underlying dynamics. The simplest model for bifurcation-induced transitions is that of a one-dimensional fold-type bifurcation [29, 31, 15]. This approach is reasonable if there is one essential component of the system experiencing negative feedback on its fast time-scale disturbances. Moreover, bifurcation theory tells us that this is one of only two possible generic one-parameter bifurcations of an attracting equilibrium, the other being the Hopf bifurcation. Close enough to such a bifurcation, one can rigorously and generically reduce the deterministic system to a one-dimensional model on a centre manifold. The negative feedback on this essential component weakens in advance of the critical transition brought about by the external change in dynamics. The resulting observational characteristic of slower and weaker responses to perturbations is called critical slowing down (CSD). If the model component undergoing such a bifurcation is a direct observable of the physical system, one can hope to employ the conventional techniques for detecting CSD, i.e. searching for positive trends in variance or lag-1 autocorrelation (AC(1)) in the time-series data. These trends are also referred to as early warning signals (EWS) in the literature, and a robust theoretical groundwork exists

*Corresponding author: andreas.morr@tum.de

[†]Earth System Modelling, School of Engineering and Design, Technical University of Munich, 80333 Munich, Germany

[‡]Complexity Science, Potsdam Institute for Climate Impact Research, 14473 Potsdam, Germany

[§]Department of Mathematics and Statistics, University of Exeter, Exeter EX4 4QF, United Kingdom

[19, 20, 22, 7]. Close to a fold-type bifurcation of a one-dimensional system whose state is denoted by $x \in \mathbb{R}$, one can approximate the dynamics by the topological normal form:

$$\dot{x}(t) = -x^2 + \alpha$$

For $\alpha > 0$, this admits one stable equilibrium at $x^*(\alpha) = \sqrt{\alpha}$ and one unstable equilibrium, whereas for $\alpha < 0$, it admits no equilibria. Linearising around the respective equilibrium point gives

$$\dot{x}(t) = -2\sqrt{\alpha}(x(t) - x^*(\alpha)) + \mathcal{O}\left((x(t) - x^*(\alpha))^2\right).$$

Adding Gaussian white noise to model the omitted fast dynamics of the original high-dimensional physical system [32, 18], the problem of determining the statistical characteristics of the process reduces to the analysis of a one-dimensional Ornstein-Uhlenbeck process:

$$\mathrm{d}X_t = -2\sqrt{\alpha}(X_t - x^*(\alpha))\mathrm{d}t + \sigma \mathrm{d}W_t,$$

where W is a Wiener process supported on the filtered probability space $(\Omega, \mathcal{F}, (\mathcal{F}_t)_{t \in \mathbb{R}_+}, \mathbb{P})$. For variance and AC(1) of the observable X, one finds in the stationary limit

$$\mathrm{Var}\left[X\right] = \frac{\sigma^2}{4\sqrt{\alpha}}, \quad \mathrm{AC}_X(1) = \exp(-2\sqrt{\alpha}),$$

which both increase as $\alpha > 0$ decreases towards the bifurcation at $\alpha = 0$.

Whether the above model simplification is valid for a given multi-dimensional physical system depends on several factors. For example, if the type of bifurcation is Hopf rather than fold, the functional expressions of variance and AC(1) will differ and may not allow for their use as EWS [8]. If the noise driving the multi-dimensional dynamics is not coupled to the centre manifold, EWS may stay silent [3]. A further complication that has not been considered previously is that even if there is a centre manifold corresponding to a fold-type bifurcation and directly impacted by white noise, the observable available for analysis need not be this component. Rather, it may be a function of multiple components of the system. Insofar as the system can be represented by a multi-dimensional random dynamical equation, we should expect the noise disturbances within the system to drive multiple components simultaneously. The alternative to such a general setup is the specific case of independent noise terms, each driving only one system component, which is an unwarranted assumption for many physical systems and can essentially be disregarded as unrealistic. We will investigate the implications of these generalisations in the context of critical slowing down. Following the previous considerations of the one-dimensional fold normal form, we proceed by introducing an uncoupled state variable y with stationary dynamics.

$$\dot{x}(t) = -x^2 + \alpha, \quad \dot{y}(t) = -y \tag{1.1}$$

This system constitutes the most reductive representation of a two-dimensional fold-type bifurcation exhibiting an abrupt transition. There is no coupling between the two deterministic equations of motion. Around the equilibrium point $(x^*(\alpha), y^*(\alpha)) = (\sqrt{\alpha}, 0)$, the linearised dynamics are

$$\begin{pmatrix}\dot{x}(t)\\ \dot{y}(t)\end{pmatrix} \approx \begin{pmatrix}-2\sqrt{\alpha} & 0\\ 0 & -1\end{pmatrix}\begin{pmatrix}x(t)-x^*(\alpha)\\ y(t)\end{pmatrix}.$$

When introducing additive white noise to this multi-dimensional setting, we are, in general, given three degrees of freedom in the form of the respective noise-couplings σ_X, σ_Y and c:

$$\begin{pmatrix}\mathrm{d}X_t\\ \mathrm{d}Y_t\end{pmatrix} = \begin{pmatrix}-2\sqrt{\alpha} & 0\\ 0 & -1\end{pmatrix}\begin{pmatrix}X_t - x^*(\alpha)\\ Y_t\end{pmatrix}\mathrm{d}t + \begin{pmatrix}\sigma_X & c\\ 0 & \sigma_Y\end{pmatrix}\begin{pmatrix}\mathrm{d}W_t^X\\ \mathrm{d}W_t^Y\end{pmatrix}$$

Note that a matrix with an additional coupling of the white noise term $\mathrm{d}W^X$ to $\mathrm{d}Y$ can always be renormalised to an upper-triangular matrix. Similarly, any third white noise term could always be represented in the above model equation containing two white noise terms. We call c the cross-coupling of the noise, which, as discussed above, will be non-zero in the general case. We will see that introducing only this additional coupling to the model can have grave implications on the ability to detect the approach of a bifurcation through conventional CSD methods. This is the – rather generic – case if the externally observable quantity is not the destabilising dimension X itself, but rather an observable $\Psi = f(X, Y)$ of the system. In general, any non-linear function f can occur as an observable. We choose the subset of linear observables as our object of study to show that the described phenomenon of failing EWS already occurs for such a simple functional relationship between the system's constituents and the observed quantity.

$$\Psi_t := \cos(\beta)X_t + \sin(\beta)Y_t \tag{1.2}$$

Eq. (1.2) covers all possible linear combinations of X and Y, and the phenomenon is impervious to an absolute scaling of the observable.

Section 2 below is dedicated to an analytical derivation of the statistical properties of Ψ and an assessment of the potential for deceitful CSD indications. Having identified possible pitfalls to the EWS in variance and AC(1) based on a linearised system, we check that those predicted behaviours indeed manifest in non-linear systems by integrating the dynamical system in Eq. (1.1) with added noise and analysing the resulting time series data in Section 3.

2. Statistical properties of the observable Ψ under linearised dynamics. To generalise the linear setting to applications beyond the particular parametrisation of the normal form given in the previous section, we now write the 2D-Ornstein-Uhlenbeck process in question generally as

$$\begin{aligned}\begin{pmatrix}\mathrm{d}X_t\\ \mathrm{d}Y_t\end{pmatrix} &= \begin{pmatrix}-\lambda_X & 0\\ 0 & -\lambda_Y\end{pmatrix}\begin{pmatrix}X_t\\ Y_t\end{pmatrix}\mathrm{d}t + \begin{pmatrix}\sigma_X & c\\ 0 & \sigma_Y\end{pmatrix}\begin{pmatrix}\mathrm{d}W_t^X\\ \mathrm{d}W_t^Y\end{pmatrix}\\ &=: A\begin{pmatrix}X_t\\ Y_t\end{pmatrix}\mathrm{d}t + \Sigma\begin{pmatrix}\mathrm{d}W_t^X\\ \mathrm{d}W_t^Y\end{pmatrix}\end{aligned} \tag{2.1}$$

The deterministic linear dynamics are still uncoupled, and we have carried along the cross-coupling c of the noise terms. Without loss of generality, we have also centred the dynamics of the X dimension around 0. In its stationary limit the zero-mean process $(X,Y)^T$ has the following covariance matrix

$$V := \mathbb{E}\left[(X_t,Y_t)^T(X_t,Y_t)\right] = \begin{pmatrix} \frac{\sigma_X^2+c^2}{2\lambda_X} & \frac{\sigma_Y c}{\lambda_X+\lambda_Y} \\ \frac{\sigma_Y c}{\lambda_X+\lambda_Y} & \frac{\sigma_Y^2}{2\lambda_Y} \end{pmatrix}$$

This can be obtained by solving the continuous-time Lyapunov equation

$$AV + VA^T + \Sigma\Sigma^T = 0.$$

Adopting the initial condition $(X_0,Y_0)^T \sim \mathcal{N}(0,V)$, the process is stationary, and the time-covariance matrix for all $\tau \geq 0$ is given by

$$R(\tau) := \mathbb{E}\left[(X_t,Y_t)^T(X_{t+\tau},Y_{t+\tau})\right] = \exp(\tau A)V$$

Note that $R(\tau)$ for $\tau \neq 0$ will in general not be a symmetric matrix, since $\mathbb{E}[X_tY_{t+\tau}] = \mathbb{E}[X_{t+\tau}Y_t]$ if and only if $c=0$ or $\lambda_X = \lambda_Y$:

$$R(\tau) = \begin{pmatrix} \frac{\sigma_X^2+c^2}{2\lambda_X}\exp(-\lambda_X|\tau|) & \frac{\sigma_Y c}{\lambda_X+\lambda_Y}\exp(-\lambda_X|\tau|) \\ \frac{\sigma_Y c}{\lambda_X+\lambda_Y}\exp(-\lambda_Y|\tau|) & \frac{\sigma_Y^2}{2\lambda_Y}\exp(-\lambda_Y|\tau|) \end{pmatrix}.$$

The same holds true for the time-correlation matrix

$$r(\tau) = \begin{pmatrix} \exp(-\lambda_X|\tau|) & \frac{2c}{\sqrt{\sigma_X^2+c^2}}\frac{\sqrt{\lambda_X\lambda_Y}}{\lambda_X+\lambda_Y}\exp(-\lambda_X|\tau|) \\ \frac{2c}{\sqrt{\sigma_X^2+c^2}}\frac{\sqrt{\lambda_X\lambda_Y}}{\lambda_X+\lambda_Y}\exp(-\lambda_Y|\tau|) & \exp(-\lambda_Y|\tau|) \end{pmatrix}$$

For any linear observable $\Psi(\beta) = \cos(\beta)X + \sin(\beta)Y$ of the 2D-system, we may now compute the variance and the autocorrelation function in the stationary limit:

$$\mathrm{Var}[\Psi] = \cos^2(\beta)V_{1,1} + \sin^2(\beta)V_{2,2} + 2\cos(\beta)\sin(\beta)V_{1,2},$$

where $V_{i,j}$ is the respective entry of the covariance matrix V. For the autocorrelation in time, we have:

$$\begin{aligned} &\mathrm{AC}_\Psi(1) := \mathbb{E}[\Psi_t\Psi_{t+\tau}]/\mathrm{Var}[\Psi] \\ &= (\cos^2(\beta)R(\tau)_{1,1} + \sin^2(\beta)R(\tau)_{2,2} + \cos(\beta)\sin(\beta)(R(\tau)_{1,2} + R(\tau)_{2,1}))/\mathrm{Var}[\Psi] \end{aligned}$$

As expected from the uncoupled nature of the deterministic dynamics, if we choose $\beta = 0$, i.e. $\Psi = X$, we essentially retrieve the conventional quantities from the one-dimensional case. Also, not surprisingly, if we only inspect the second dimension $\Psi = Y$, the variance and AC(1) will not depend on the destabilisation of X, i.e. $\lambda_X \to 0$, and can not function as EWS. See Table 1 for explicit expressions.

Table 1: Edge cases of the linear observable setting. The conventional EWS information is perfectly conserved in the first case and entirely lost in the second.

β	Ψ	$\mathrm{Var}[\Psi]$	$\mathrm{AC}_\Psi(1)$
0	X	$(\sigma_X^2 + c^2)/2\lambda_X$	$\exp(-\lambda_X)$
$\pi/2$	Y	$\sigma_Y^2/2\lambda_Y$	$\exp(-\lambda_Y)$

In all other cases, the observable Ψ consists of some amplitude of X and Y, i.e. $\beta \neq k\pi/2$ for $k \in \mathbb{Z}$. Even here, the EWS seem to be reliable at first glance. We have

$$\mathrm{Var}[\Psi] \xrightarrow{\lambda_X \to 0} \infty, \quad \mathrm{AC}_\Psi(1) \xrightarrow{\lambda_X \to 0} 1.$$

These increases are monotonic in proximity to the bifurcation, where $\lambda_X = 0$. More precisely, for any parameter setting $\lambda_Y > 0$, $\sigma_X > 0$, $\sigma_Y > 0$ and $c \geq 0$, there exists a $\lambda_X^* > 0$ with the property that both variance and AC(1) are monotonically increasing as λ_X decreases from λ_X^* to 0. In that sense, there still is a time span in the advent of the fold-type bifurcation, in which the linearised dynamics predict a clear increase in both variance and AC(1), making them applicable as EWS in this case.

However, the practical caveat to this finding is the value of λ_X^* and the behaviour of the EWS before this threshold. We give the following example, which illustrates that using EWS has potential pitfalls and may lead to a misinterpretation of the actual destabilisation in the underlying dynamics. For this, choose $\lambda_Y = 1$, $\sigma_X = 0.1$, $\sigma_Y = 2$ and $c = 1$, meaning

$$\begin{pmatrix} \mathrm{d}X_t \\ \mathrm{d}Y_t \end{pmatrix} = \begin{pmatrix} -\lambda_X & 0 \\ 0 & -1 \end{pmatrix} \begin{pmatrix} X_t \\ Y_t \end{pmatrix} \mathrm{d}t + \begin{pmatrix} 0.1 & 1 \\ 0 & 2 \end{pmatrix} \begin{pmatrix} \mathrm{d}W_t^X \\ \mathrm{d}W_t^Y \end{pmatrix}, \tag{2.2}$$

and examine the observable $\Psi(\beta)$ associated with the mixing angle $\beta = -\frac{\pi}{4}$, i.e. $\Psi_t = 2^{-1/2}(X_t - Y_t)$. Figure 1 shows the variance and AC(1) of Ψ as a function of the destabilising eigenvalue λ_X. Although the expected increasing behaviour can be observed when decreasing λ_X from $\lambda_X^* \approx 0.6$ towards 0, both CSD indicators, in fact, decrease as long as λ_X decreases toward λ_X^*. It is this veiling of the critical slowing down of the X dimension that we would like to point out in this work.

The underlying prerequisite of the phenomenon explored above is the following configuration: The noise component $\mathrm{d}W^Y$ is positively coupled to both dimensions of the deterministic dynamics. At the same time, the observable Ψ is defined such that the two linear components have opposing signs. This leads to the disturbances in X and Y interfering with each other in the summary observable Ψ. We show with the following Lemma that this effect is ubiquitous with respect to the specific parameter choices.

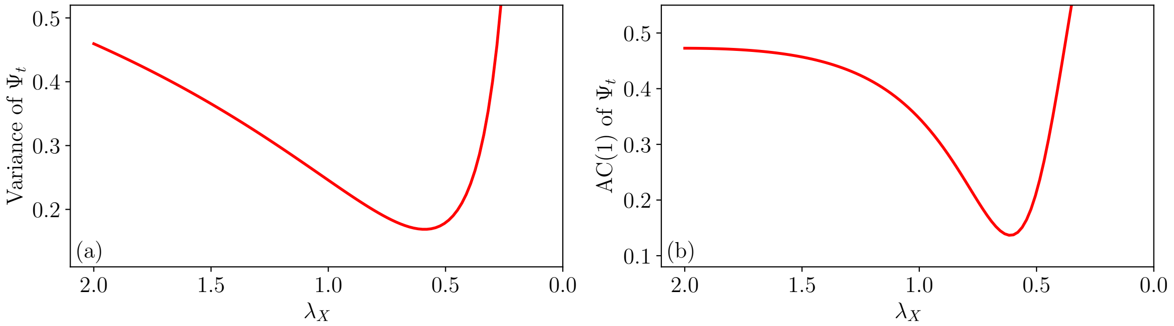

Figure 1: **(a)** Variance and **(b)** AC(1) of the observable Ψ for $\beta = -\frac{\pi}{4}$ in the linearised setting described in the main text. While these two classical CSD indicators ultimately increase to their expected limits ∞ and 1 respectively as $\lambda_X \to 0$, the behaviour up until that increase can be deceitful with respect to critical slowing down.

Lemma 2.1. *Consider the linear stochastic differential equation (2.1) with non-zero constants λ_Y, σ_X, σ_Y and c. There exists an open interval of observation angles $\beta \in (\beta^1, \beta^2)$ for which both variance and AC(1) of Ψ defined through Eq. (1.2) decrease with a decreasing $\lambda_X \in (\lambda_X^1, \lambda_X^2)$.*

Proof. We can find such an interval of observation angles $\beta \in (\beta^1, \beta^2)$ close to the choice $\Psi = Y$, i.e. $\beta = \pi/2$. We have already derived analytical expressions of $\mathrm{Var}[\Psi]$ and $\mathrm{AC}_\Psi(1)$. They are smooth functions of the system's parameters. The quantities decrease with a decreasing λ_X if their partial derivative with respect to λ_X is positive. We find at the trivial choice of $\Psi = Y$ that for all $\lambda_X \in \mathbb{R}$

$$\partial_{\lambda_X} \mathrm{Var}[\Psi]\Big|_{\beta=\pi/2} = 0 \quad \text{and} \quad \partial_{\lambda_X} \mathrm{AC}_\Psi(1)\Big|_{\beta=\pi/2} = 0 \tag{2.3}$$

Furthermore, we find that the derivative of these quantities with respect to the observation angle β is non-zero and equal in sign for both of the quantities when choosing $\lambda_X = \lambda_Y$:

$$\partial_\beta \partial_{\lambda_X} \mathrm{Var}[\Psi]\Big|_{\beta=\pi/2,\, \lambda_X=\lambda_Y} = -\frac{c\sigma_Y}{2\lambda_Y^2} \quad \text{and} \quad \partial_\beta \partial_{\lambda_X} \mathrm{AC}_\Psi(1)\Big|_{\beta=\pi/2,\, \lambda_X=\lambda_Y} = -\frac{ce^{-\lambda_Y}}{\sigma_Y}$$

Depending on the signs of c and σ_Y, there will be an interval $(\pi/2, \beta_2)$ or $(\beta_1, \pi/2)$ for which the quantities of Eq. (2.3) are positive at $\lambda_X = \lambda_Y$. Since these two quantities are continuous in λ_X, they will also be positive for all λ_X in an interval $(\lambda_Y - \delta, \lambda_Y + \delta)$. This concludes the proof. Note that the chosen interval is not the only region for which the phenomenon discussed in this work is prevalent (see Figure 2c). □

The Lemma implies that, as long as we have a cross-coupling $c \neq 0$, the phenomenon persists for all generic choices of σ_X, σ_Y, c and λ_Y. On the other hand, the extent to which it quantitatively inhibits the use of EWS in an application setting will heavily depend on these values. Giving a general guideline of which configurations exhibit a lengthy and pronounced decrease in variance and AC(1), even though CSD would imply an increase, is not feasible given the number of degrees of freedom. We provide a Python script with which the prevalence of the effect can be assessed for different parametrisations. Central to this script is the radial plotting of the approach to the critical value $\lambda_X^{\text{crit}} = 0$ from different angles β (see Figure 2 and its description).

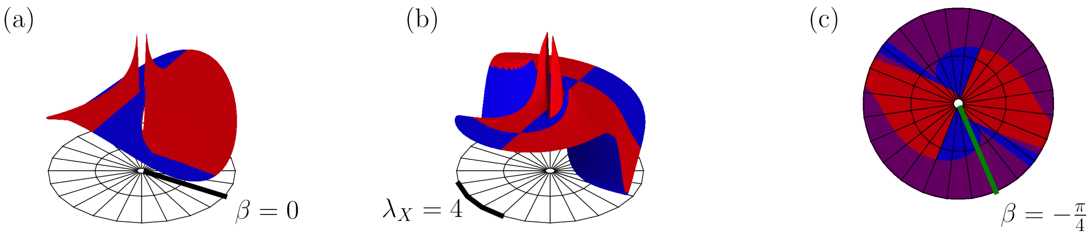

Figure 2: Contour plot of **(a)** the variance and **(b)** AC(1) for different values of β and λ_X in the 2D-Ornstein-Uhlenbeck setting of (2.2). The distance from the centre constitutes the value of λ_X while the angle around the circle is β. The radius of the plots and, therefore, the maximal value of λ_X is 4. The second concentric circle marks $\lambda_X = 2$. The colour of the contour plot is red where the radial derivative of the respective quantity towards the centre is positive and blue where it is negative. In this sense, all blue regions represent the angles β and values of λ_X where deceitful CSD indications are prevalent. Figure **(c)** is a top-down view of the two contour plots. The blue and red regions are those where variance and AC(1) agree on the respective trend. In the purple regions, the trends disagree. The green line shows the trajectory towards the middle for a fixed $\beta = -\frac{\pi}{4}$, meaning from the second circle on, it is the same line as plotted in Figure 1 for variance and AC(1), respectively.

3. Observations in model data. After identifying potential pitfalls to employing variance and AC(1) on linear observables of the linearised system, we test these predictions on synthetic data of the true fold bifurcation in Eq. (1.1). To this end, we integrate the following system of stochastic differential equations using the Euler-Mayurama scheme.

$$\begin{aligned} \begin{pmatrix} \mathrm{d}X_t \\ \mathrm{d}Y_t \end{pmatrix} &= \begin{pmatrix} -X_t^2 + \alpha(t) \\ -Y_t \end{pmatrix} \mathrm{d}t + \varepsilon \begin{pmatrix} 0.1 & 1 \\ 0 & 2 \end{pmatrix} \begin{pmatrix} \mathrm{d}W_t^X \\ \mathrm{d}W_t^Y \end{pmatrix} \\ \alpha(t) &= 1 - \frac{11}{10}\frac{t}{T} \end{aligned} \tag{3.1}$$

Over the time span of $T = 10^4$, this integration is performed at a time-step of $\delta t = 1/30$ and subsequently sampled at every 30th value. In order to ensure that premature noise-induced tipping is restricted to a relatively short period before the bifurcation, we introduce the noise-scaling parameter $\varepsilon = 0.1$. For better illustration, we artificially introduce a second stable state for X past the bifurcation point. These dynamics are omitted in the SDE (3.1). The results for the linear observable

$$\Psi_t = \cos(\beta)X_t + \sin(\beta)Y_t = \frac{1}{\sqrt{2}}(X_t - Y_t)$$

with $\beta = -\frac{\pi}{4}$ are given in Figure 3. Even though the dynamics are now non-linear and non-autonomous, the contemporary linearised system still allows for a good assessment of the expected time-series statistics. The corresponding estimators of variance and AC(1) indeed give the expected results. The quantities decrease with time, even though the destabilisation of the system in the dimension of the X component should conventionally incur an increase. The interference of the shared driving noise in the linear observable Ψ constitutes a break with the necessary modelling assumptions for CSD detection via variance and AC(1) in a single observable. Note that similarly, a stabilisation of the system, i.e. an increase in λ_X, would cause the variance and AC(1) to increase. This is a setting in which a false alarm with respect to CSD would be raised.

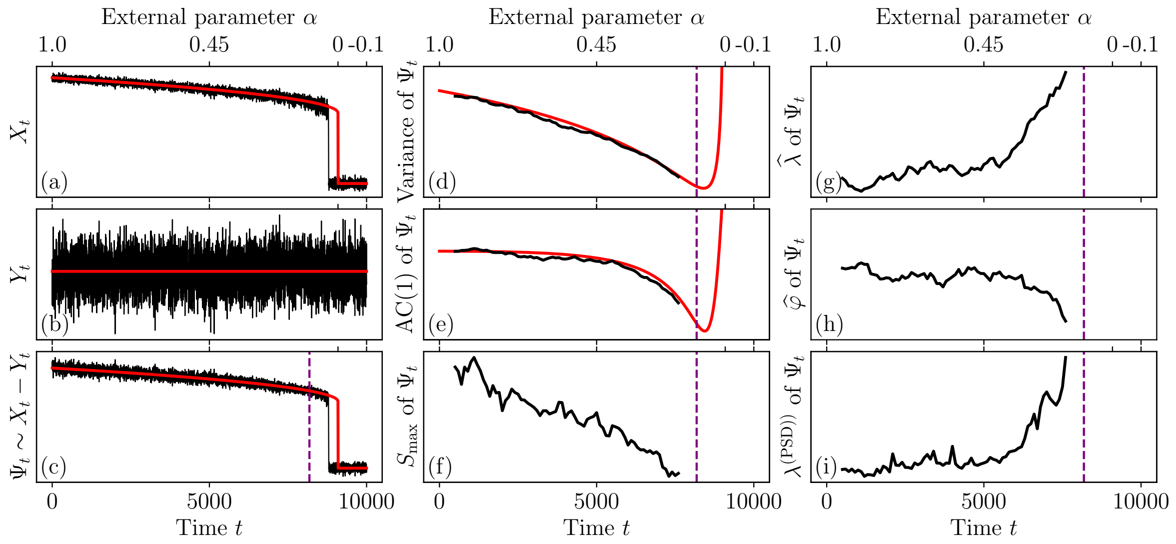

Figure 3: **(a) - (c)** Sample paths of X_t, Y_t and Ψ_t following the SDE (3.1) in the main text with $\beta = -\frac{\pi}{4}$. Up until the purple dashed line, after which noise-induced tipping may frequently come into play, the variance and AC(1) of Ψ are each estimated over windows of length $N = 1000$. The averaged results over 10 runs are plotted in **(d)** and **(e)** respectively, along with their theoretically computed values from considerations of the linearised model. Their decrease would be misinterpreted as a stabilisation of the system rather than an approach of an abrupt transition. In **(f) - (i)**, alternative indicators for CSD are calculated. These are **(f)** the maximum of the observed power spectral density (PSD) [8], **(g)** the linear restoring rate estimated through a Langevin approach [25], **(h)** a generalised least squares estimator for an AR(1) model [4] and **(i)** the linearised restoring rate estimated via the PSD [24]. These quantities, too, exhibit the respective opposite trend of what would be expected of a destabilising system.

4. Discussion. We consider a generic fold-type bifurcation in a class of multi-dimensional dynamical systems, where we assume that noise drives multiple components of the system. We demonstrate that such a setup can easily produce observables that, because of internal noise interference, exhibit deceiving trends in variance and lag-1 autocorrelation with respect to CSD. Such false or missed alarms have been shown to be an issue in systems driven by non-stationary or non-white noise [14, 21, 4, 7, 27, 24, 25] or systems exhibiting deterministic coupling [8, 3]. It has also been shown that a misrepresentation of the natural system as a fold-type bifurcation with direct noise influence [17, 11] or issues with the availability of time series data [13, 2, 30] may lead to similar problems. This work introduces a previously unknown complication with the detection of CSD via variance and AC(1), as well as other techniques [8, 25, 4, 24, 10] (see also Figure 3f-i). Even though the severity of the effect described here depends heavily on the relative values of the systems restoring rates and noise couplings, its presence is ubiquitous (see Lemma 2.1). Furthermore, if present, the effect can only be ruled out by choice of a different observable Ψ, which is often not achievable in the observations of natural systems.

Whenever possible, a sufficient physical understanding and previous model validation should confirm that the conventional assumption of a directly observed noisy dynamical system along its centre manifold is warranted. In this case, the presented results do not call into question the expressiveness of the conventional EWS.

Data Availability. Visit the GitHub repository LinearObservablesCSD to access the code used to generate all figures in this manuscript.

Acknowledgments. This work has received funding from the Volkswagen Stiftung, the European Union's Horizon 2020 research and innovation programme under grant agreement No. 820970 and under the Marie Sklodowska-Curie grant agreement No. 956170, as well as from the Federal Ministry of Education and Research under grant No. 01LS2001A. This is TiPES contribution #X.

REFERENCES

[1] P. Ashwin, S. Wieczorek, R. Vitolo, and P. Cox, *Tipping points in open systems: Bifurcation, noise-induced and rate-dependent examples in the climate system*, Philosophical Transactions of the Royal Society A: Mathematical, Physical and Engineering Sciences, 370 (2012), pp. 1166–1184, https://doi.org/10.1098/rsta.2011.0306.

[2] M. Ben-Yami, V. Skiba, S. Bathiany, and N. Boers, *Uncertainties in critical slowing down indicators of observation-based fingerprints of the Atlantic Overturning Circulation*, 2023.

[3] M. C. Boerlijst, T. Oudman, and A. M. de Roos, *Catastrophic collapse can occur without early warning: Examples of silent catastrophes in structured ecological models*, PLOS ONE, 8 (2013), pp. 1–6, https://doi.org/10.1371/journal.pone.0062033.

[4] N. Boers, *Observation-based early-warning signals for a collapse of the Atlantic Meridional Overturning Circulation*, Nature Climate Change, 11 (2021), pp. 680–688, https://doi.org/10.1038/s41558-021-01097-4.

[5] N. Boers, M. Ghil, and T. F. Stocker, *Theoretical and paleoclimatic evidence for abrupt transitions in the Earth system*, Environmental Research Letters, 17 (2022), p. 093006, https://doi.org/10.1088/1748-9326/ac8944.

[6] N. Boers, N. Marwan, H. M. J. Barbosa, and J. Kurths, *A deforestation-induced tipping point for the South American monsoon system*, Scientific Reports, 7 (2017/01/25, 2017), p. 41489, https:

//doi.org/10.1038/srep41489.
[7] C. Boettner and N. Boers, *Critical slowing down in dynamical systems driven by nonstationary correlated noise*, Physical Review Research, 4 (2022), p. 013230, https://doi.org/10.1103/PhysRevResearch.4.013230.
[8] T. M. Bury, C. T. Bauch, and M. Anand, *Detecting and distinguishing tipping points using spectral early warning signals*, Journal of The Royal Society Interface, 17 (2020), p. 20200482, https://doi.org/10.1098/rsif.2020.0482.
[9] T. M. Bury, R. I. Sujith, I. Pavithran, M. Scheffer, T. M. Lenton, M. Anand, and C. T. Bauch, *Deep learning for early warning signals of tipping points*, Proceedings of the National Academy of Sciences, 118 (2021), p. e2106140118, https://doi.org/10.1073/pnas.2106140118.
[10] J. J. Clarke, C. Huntingford, P. D. L. Ritchie, and P. M. Cox, *Seeking more robust early warning signals for climate tipping points: The ratio of spectra method (ROSA)*, Environmental Research Letters, 18 (2023), p. 035006, https://doi.org/10.1088/1748-9326/acbc8d.
[11] V. Dakos, E. H. van Nes, P. D'Odorico, and M. Scheffer, *Robustness of variance and autocorrelation as indicators of critical slowing down*, Ecology, 93 (2012), pp. 264–271, https://doi.org/10.1890/11-0889.1.
[12] P. Ditlevsen and S. Ditlevsen, *Warning of a forthcoming collapse of the Atlantic meridional overturning circulation*, Nature Communications, 14 (2023/07/25, 2023), p. 4254, https://doi.org/10.1038/s41467-023-39810-w.
[13] P. D. Ditlevsen and S. J. Johnsen, *Tipping points: Early warning and wishful thinking*, Geophysical Research Letters, 37 (2010), https://doi.org/10.1029/2010GL044486.
[14] P. S. Dutta, Y. Sharma, and K. C. Abbott, *Robustness of early warning signals for catastrophic and non-catastrophic transitions*, Oikos (Copenhagen, Denmark), 127 (2018), pp. 1251–1263, https://doi.org/10.1111/oik.05172.
[15] V. Guttal and C. Jayaprakash, *Impact of noise on bistable ecological systems*, Ecological Modelling, 201 (2007), pp. 420–428, https://doi.org/10.1016/j.ecolmodel.2006.10.005.
[16] P. O. Hopcroft and P. J. Valdes, *Paleoclimate-conditioning reveals a North Africa land-atmosphere tipping point*, Proceedings of the National Academy of Sciences, 118 (2021), p. e2108783118, https://doi.org/10.1073/pnas.2108783118.
[17] S. Kéfi, V. Dakos, M. Scheffer, E. H. Van Nes, and M. Rietkerk, *Early warning signals also precede non-catastrophic transitions*, Oikos (Copenhagen, Denmark), 122 (2013), pp. 641–648, https://doi.org/10.1111/j.1600-0706.2012.20838.x.
[18] D. Kelly and I. Melbourne, *Deterministic homogenization for fast–slow systems with chaotic noise*, Journal of Functional Analysis, 272 (2017), pp. 4063–4102, https://doi.org/10.1016/j.jfa.2017.01.015.
[19] C. Kuehn, *A mathematical framework for critical transitions: Bifurcations, fast–slow systems and stochastic dynamics*, Physica D: Nonlinear Phenomena, 240 (2011), pp. 1020–1035, https://doi.org/10.1016/j.physd.2011.02.012.
[20] C. Kuehn, *A mathematical framework for critical transitions: Normal forms, variance and applications*, Journal of Nonlinear Science, 23 (2013/06/01, 2013), pp. 457–510, https://doi.org/10.1007/s00332-012-9158-x.
[21] C. Kuehn, K. Lux, and A. Neamţu, *Warning signs for non-Markovian bifurcations: Colour blindness and scaling laws*, Proceedings of the Royal Society A: Mathematical, Physical and Engineering Sciences, 478 (2022), p. 20210740, https://doi.org/10.1098/rspa.2021.0740.
[22] T. M. Lenton, V. N. Livina, V. Dakos, E. H. van Nes, and M. Scheffer, *Early warning of climate tipping points from critical slowing down: Comparing methods to improve robustness*, Philosophical Transactions of the Royal Society A: Mathematical, Physical and Engineering Sciences, 370 (2012), pp. 1185–1204, https://doi.org/10.1098/rsta.2011.0304.
[23] C. Meisel, A. Klaus, C. Kuehn, and D. Plenz, *Critical slowing down governs the transition to neuron spiking*, PLOS Computational Biology, 11 (2015), pp. 1–20, https://doi.org/10.1371/journal.pcbi.1004097.
[24] A. Morr and N. Boers, *Detection of approaching critical transitions in natural systems driven by red noise*, 2023.
[25] A. Morr, K. Riechers, L. R. Gorjão, and N. Boers, *Anticipating critical transitions in multi-dimensional systems driven by time- and state-dependent noise*, 2023.

[26] F. Nazarimehr, S. Jafari, M. Perc, and J. C. Sprott, *Critical slowing down indicators*, Europhysics Letters, 132 (2020), p. 18001, https://doi.org/10.1209/0295-5075/132/18001.

[27] D. Proverbio, A. Skupin, and J. Gonçalves, *Systematic analysis and optimization of early warning signals for critical transitions using distribution data*, iScience, 26 (2023), p. 107156, https://doi.org/10.1016/j.isci.2023.107156.

[28] H. Ren and D. Watts, *Early warning signals for critical transitions in power systems*, Electric Power Systems Research, 124 (2015), pp. 173–180, https://doi.org/10.1016/j.epsr.2015.03.009.

[29] M. Scheffer, J. Bascompte, W. A. Brock, V. Brovkin, S. R. Carpenter, V. Dakos, H. Held, E. H. van Nes, M. Rietkerk, and G. Sugihara, *Early-warning signals for critical transitions*, Nature, 461 (2009), pp. 53–59, https://doi.org/10.1038/nature08227.

[30] T. Smith, R.-M. Zotta, C. A. Boulton, T. M. Lenton, W. Dorigo, and N. Boers, *Reliability of resilience estimation based on multi-instrument time series*, Earth System Dynamics, 14 (2023), pp. 173–183, https://doi.org/10.5194/esd-14-173-2023.

[31] J. M. T. Thompson and J. Sieber, *Climate tipping as a noisy bifurcation: A predictive technique*, IMA Journal of Applied Mathematics, 76 (2010), pp. 27–46, https://doi.org/10.1093/imamat/hxq060.

[32] R. Zwanzig, *Nonequilibrium Statistical Mechanics*, Oxford University Press, 2001.